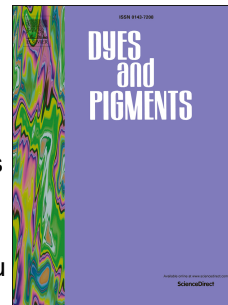


# Accepted Manuscript

A curcumin-based NIR fluorescence probe for detection of amyloid-beta ( $A\beta$ ) plaques in Alzheimer's disease

Guofu Si, Shujie Zhou, Guoyong Xu, Jiafeng Wang, Baoxing Wu, Shuangsheng Zhou



PII: S0143-7208(18)31991-0

DOI: <https://doi.org/10.1016/j.dyepig.2018.12.003>

Reference: DYPI 7208

To appear in: *Dyes and Pigments*

Received Date: 8 September 2018

Revised Date: 4 December 2018

Accepted Date: 5 December 2018

Please cite this article as: Si G, Zhou S, Xu G, Wang J, Wu B, Zhou S, A curcumin-based NIR fluorescence probe for detection of amyloid-beta ( $A\beta$ ) plaques in Alzheimer's disease, *Dyes and Pigments* (2019), doi: <https://doi.org/10.1016/j.dyepig.2018.12.003>.

This is a PDF file of an unedited manuscript that has been accepted for publication. As a service to our customers we are providing this early version of the manuscript. The manuscript will undergo copyediting, typesetting, and review of the resulting proof before it is published in its final form. Please note that during the production process errors may be discovered which could affect the content, and all legal disclaimers that apply to the journal pertain.

**A curcumin-based NIR fluorescence probe for detection of amyloid-beta (A $\beta$ )  
plaques in Alzheimer's Disease**

Guofu Si <sup>a</sup>, Shujie Zhou <sup>b</sup>, Guoyong Xu <sup>c</sup>, Jiafeng Wang <sup>a</sup>, Baoxing Wu <sup>a, c</sup>,  
Shuangsheng Zhou <sup>a, c</sup> \*

<sup>a</sup> *Department of Pharmacy, Anhui University of Chinese Medicine, Hefei 230012,  
P.R.China*

<sup>b</sup> *Qilu school of Medicine, Shandong University, Jinan 502100, P.R. China*

<sup>c</sup> *Institute of Physical Science and Information Technology, Anhui University, Hefei  
230601, P.R.China*

**Abstract:** Amyloid-beta (A $\beta$ ) peptide as one of the main components of senile plaques is closely related to the onset and progression of incurable Alzheimer's disease (AD). In recent years, it is reported that curcumin derivatives have been used as the near-infrared (NIR) fluorescence imaging probes of A $\beta$  plaques for the early diagnosis of AD. To further develop a curcumin-based NIR fluorescent probe for A $\beta$  plaques, in this work, we have synthesized three novel curcumin-based NIR Dyes. Among them, the curcumin derivative Dye 2 showed a significant enhancement in its fluorescence intensity ( $\lambda_{em}$ , 635 nm; 19.5-fold increase in quantum yield,  $\Phi = 0.36$ ;  $K_d$ , 1.13  $\mu$ M) after binding to A $\beta$  plaques. Additionally, *in vitro* and *in vivo* fluorescence imaging of A $\beta$  plaques stained with Dye 2 confirmed that the compound was a potential probe to detect A $\beta$  plaques in AD. This work opens a perspective to rationally design novel curcumin-based NIR compound for A $\beta$  detection.

**Keywords:** Curcumin, NIR fluorescence probe, Amyloid-beta deposits, Fluorescence imaging, Amyloid-beta plaques, Alzheimer's Disease

## 1. Introduction

Alzheimer's disease (AD) is the most common form of dementia in the elderly.

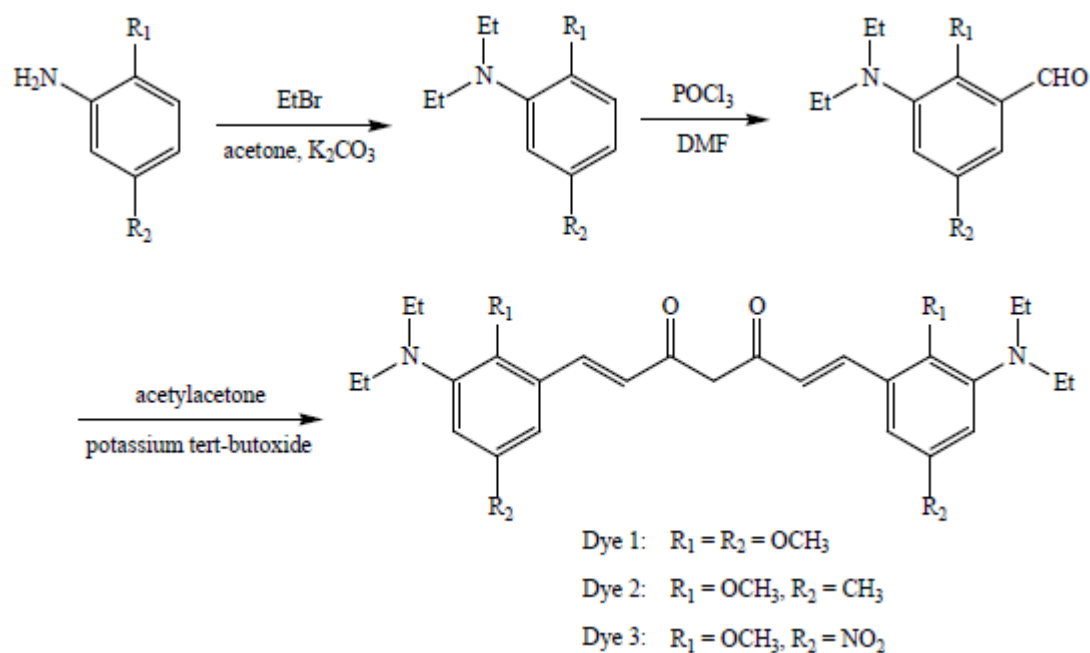
Pathologically, AD is a neurodegenerative disease characterized by extracellular senile plaques consisting of fibrillar amyloid-beta ( $A\beta$ ) peptides. The formation of neurofibrillary tangles (NFTs) eventually results in neurodegeneration and brain atrophy. Furthermore, deposition of  $A\beta$  is considered to be the most important pathophysiological hallmark of AD according to the amyloid-cascade hypothesis [1]. The diagnosis of AD has increasingly become the focus of attention in recent years. Currently, memory and behavioral tests are widely used for late-stage AD diagnosis [2]. Up to now, computer image techniques, including computed tomography (CT), magnetic resonance imaging (MRI), positron emission tomography (PET) and so on, have been employed for the early detection of AD pathology, and considerable progress has been achieved [3–13]. However, these computer imaging techniques also showed some limitations, such as high cost, lack of sensitivity, involvement of radioactive compounds and sophisticated instrumentation as well as data analysis variability. On the contrary, fluorescence imaging, particularly near-infrared (NIR) probe has appeared to be an attractive alternative as a simple, inexpensive and rapid technique that allows real-time monitoring of the  $A\beta$  aggregation in a sensitive and high-resolution manner.

The NIR fluorescence imaging provides enormous potential as a noninvasive method for *in vivo* imaging because biomolecules have low absorption and autofluorescence in the NIR (>630 nm), which result in an optimal penetration depth and high sensitivity, thus there has been an increasing demand for new chemical materials that can be used as NIR fluorescence probes for the early detection of  $A\beta$  plaques and interneuronal deposits of NFTs in AD. It is generally accepted that good NIR probes for the detection of  $A\beta$  plaques should have the following fundamental characteristics: 1) specificity to  $A\beta$  plaques; 2) emission wavelength > 630 nm and a large Stokes shift; 3) low cytotoxicity for *in vivo* imaging; 4) high quantum yield and affinity binding; 5) reasonable stability in blood.

Curcumin is a natural yellow pigment that is derived from the rhizomes of *Curcuma longa*. Besides its effective antioxidant, anti-inflammatory, antimicrobial

and antiviral properties, the compound is also considered as a cancer chemopreventive agent [14,15]. Additionally, curcumin and its derivatives have been reported to possess good optical and electrical properties because of a highly  $\pi$ -electron delocalized and symmetric structure [16,17]. Besides, curcumin has recently been recognized as a fluorescence probe for the *in vivo* visualization of both A $\beta$  plaques and intraneuronal deposits of NFTs [18,19]. However, the practical use of curcumin as a NIR probe is limited due to its fluorescence emission wavelength ( $< 530$  nm) [20], which is outside the NIR range. To induce a red-shift of the fluorescence emission wavelength, a compound with a push/pull electron architecture is generally designed by introducing terminal electron-rich donor or electron-deficient acceptor groups to a highly  $\pi$ -conjugated structure system according to principle of Marder [21] and Perry [22]. For instance, curcumin derivatives (e.g. CRANAD-2, CRANAD-6, CRANAD-17 and CRANAD-58) with push/pull structures have been devised and prepared by Anna Moore [23] as NIR fluorescence probes for the *in vivo* imaging of AD pathology. Those compounds show fluorescence emission in the NIR range, high affinity to A $\beta$ , and better fluorescence properties (considerable increase in fluorescence intensity, large Stokes shift and high quantum yield) upon binding to A $\beta$  aggregates.

We are interested in searching novel curcumin-based molecular probes that can be used for the NIR fluorescence imaging of A $\beta$  plaques. For this purpose, in the paper, three new curcumin derivatives, 1,7-bis[(2,5-dimethoxy-3-diethylamino)phenyl]-1,6-heptadiene--3,5-dione (Dye 1), 1,7-bis[(2-methoxy-3-diethylamino-5-methyl)phenyl]-1,6-heptadiene--3,5-dione (Dye 2) and 1,7-bis[(2-methoxy-3-diethylamino-5-nitryl)phenyl]-1,6-heptadiene--3,5-dione (Dye 3), were synthesized. Simultaneously, the photophysical and cytotoxic properties of these compounds were also investigated. Additionally, the application of the Dye 2 as an *in vitro* and *in vivo* NIR fluorescent probe for the imaging of A $\beta$  plaques was primarily studied. The synthetic route of Dyes 1-3 is presented in Scheme 1.



**Scheme 1** Synthetic route of as-prepared Dyes 1-3

## 2. Materials and methods

### 2.1. Materials and general instruments

All chemicals were available commercially and every solvent was purified by conventional methods before use. Monomeric  $A\beta_{1-40}$  was purchased from r-Peptide (GA, USA). Double distilled water was used throughout all experiments. All compounds were first dissolved in DMSO to 2 mM, and then diluted by phosphate buffer solution (PBS, pH = 7.2, Gibco) to different concentration. Each solution used for photophysical properties was freshly prepared and kept in the dark before measurement. All aqueous solutions were prepared in distilled water. AD patients brain frozen tissue (83 years old) and paraffin brain sections were obtained China Pharmaceutical University (Nanjing, China) with the permission for the use of tissue and clinical information for research purposes.

Melting points were determined on WRS-2 (Shanghai China).  $^1\text{H}$  NMR and  $^{13}\text{C}$  NMR spectra were performed on a Bruker 400 spectrometer with tetramethylsilane ( $\text{Si}(\text{CH}_3)_4$ ) as the internal standard. The mass spectra were obtained on FINNIGAN LCQ Advantage MAX LC/MS (Thermo Finnigan, American). Elemental analysis was carried out with a Perkin-Elmer 240C analyzer.

## 2.2. Photophysical methods

Absorbance spectra were obtained on a Shimadzu UV-1650 PC spectrophotometer (Shimadzu, Sydney NSW) and emission spectra were obtained on a Varian CAREY Eclipse fluorescence spectrophotometer (Varian, California USA). The quartz cuvettes used with a 1 cm path length were used for all spectral collection. The fluorescence quantum yields of target compounds in DMF were measured according to literature [14].

## 2.3. Preparation of A $\beta$ <sub>1-40</sub> plaques and measurement of their binding constants

The preparation of A $\beta$ <sub>1-40</sub> plaques was carried out according to the method reported previously [24]. In brief, A $\beta$ <sub>1-40</sub> monomer was diluted to 50  $\mu$ M with PBS (pH = 7.2) and incubated at 37 °C for 3 days. TEM formation of A $\beta$ <sub>1-40</sub> plaques..

The *in vitro* binding constants of Dyes 1-3 with A $\beta$ <sub>1-40</sub> plaques were determined as below. A solution of A $\beta$  plaques (a final concentration of 50  $\mu$ M) was mixed with different concentrations of each Dye (0, 20, 40, 60, 80 and 100  $\mu$ M) and incubated at room temperature for 5 min. Emission spectra of the resultant mixture were measured by a fluorescence spectrometer. The apparent dissociation constants ( $K_d$ ) resulted from the saturation experiments were calculated by software Prism 3.0 with nonlinear one-site binding regression.

## 2.4. Cytotoxicity and stability in mouse plasma experiments

The cytotoxic effects of the obtained compound were assessed using the MTT assay. Human breast cancer (MCF-7) cell lines were seeded into a 96-well culture plate at about  $1.0 \times 10^5$  cell/well. 50  $\mu$ L of the sample solution diluted with DMEM at different concentrations was added to each well, respectively. The cells were cultivated for 24 h at 37 °C, 5% CO<sub>2</sub> and 95% air, followed by the addition of 50  $\mu$ L MTT solution (5 mg/mL) to each well and incubated for an additional 2 h (37 °C, 5% CO<sub>2</sub> and 95% air). Then, DMEM was removed, the cells were dissolved in DMSO (150  $\mu$ L/well), the absorbance was determined by UV spectrometer at 540 nm. The percentage of cell viabilities was calculated by the following equation: cell viability (%) = (OD<sub>treated</sub>/OD<sub>control</sub>)  $\times$  100%, where OD<sub>treated</sub> was obtained in the presence of sample at various concentration, OD<sub>control</sub> was obtained from the incubation medium.

Three independent trials were conducted, and the average percentage of viable cells was calculated relative to untreated cells[25].

Normal Kunming mice were purchased from Animal Laboratory of China Pharmaceutical University (Nanjing, China). All animal experiments were performed in compliance with the Animal Management Rules of the Ministry of Health of the People's Republic of China. The *in vitro* stabilities of Dyes 1-3 in mouse plasma were determined as follows. After peritoneal injection of pentobarbital sodium ( $40 \text{ mg kg}^{-1}$ ), plasma samples were drawn from cardiac puncture of the mouse and mixed with heparin (China) to prevent clotting. Each dye was added to the mouse plasma ( $400 \mu\text{L}$ ), and the plasma samples were incubated at  $37^\circ\text{C}$  for 1 h. After incubation, plasma samples were mixed with equal volumes of acetonitrile, followed by centrifugation for 10 min to remove the denatured proteins. The supernatant was filtrated using a  $0.50 \mu\text{m}$  filter (Millipore; Billerica, MA, USA). Then, the filtrate was collected and determined at different time points by fluorescence spectrometer.

## **2.5. AD patients brain tissue sections staining**

Dye 2 was selectively used for bioimaging studies because of low cytotoxicity, strong fluorescence intensity, high quantum yield and binding to  $\text{A}\beta$  plaques. The paraffin tissue of AD patients was sliced into  $5 \mu\text{m}$  by a microtome (Leica RM2235, Germany). The paraffin brain sections were washed with xylene, 80% ethanol solutions and PBS ( $\text{pH} = 7.2$ ), respectively. Auto fluorescence of the tissue was quenched using potassium permanganate (0.20% in PBS) for 20 min, followed by washing with PBS, then the sections were washed with potassium metbisulfite (1%) and oxalic acid (1%) until the brown color was removed, and then washed with PBS. The sections were stained with Dye 2 ( $20 \mu\text{M}$ ) for 1 h, washed by PBS three four times to remove unlabeled molecules, and sealed with 80% glycerin and coverslips. The sections were imaged using a fluorescence microscope (Olympus IX81, Tokyo, Japan) and a SPOT digital camera (Diagnostic Instruments, USA). Under the same condition, the adjacent section was also stained with silver reagent, a pathological dye commonly used for staining  $\text{A}\beta$  plaques in the brain [26].

## **2.6. In vivo NIR imaging**

In *in vivo* imaging studies were carried out with the IVIS Lumina system (Xenogen Co., Alameda, CA, USA) following the reported procedure [27-29]. The images were acquired with a 600 nm excitation filter and a 680 nm emission filter. Data analyses were performed using the KodakTM1D Analysis software.

Mice (n = 4 for APP/PSI transgenic mice) were shaved before background imaging, and each mouse was intravenously injected with solution of Dye 2 (3.0 mg/kg, 20% DMSO, 80% PBS). Fluorescence signals from the brain were recorded at 0 h, 1.0 h, 2.0 h, 3.0 h and 4.0 h after injection of the compound Dye 2.

## 2.7. Preparation of compounds

**2,5-dimethoxy-N,N-diethylamino.** 2,5-dimethoxyaniline (0.61 g, 4.0 mM) and 20 mL of acetone solution containing anhydrous potassium carbonate (1.2 g, 8.2 mM) and bromoethane (0.5 mL) were added into a round-bottom flask equipped with a magnetic stirrer. The resultant mixture was stirred for 15 h at 80 °C, cooled to RT, and then filtered. The crude product was purified by column chromatography (ethyl acetate : petroleum ether mixture = 3:2) to give a 2,5-dimethoxy-N,N-dimethylaniline as colorless powder. Yield: 61.3%.

**2,5-dimethoxy-3-diethylaminobenzaldehyde.** 5 mL of dry DMF was cooled to 0 °C and treated dropwise with POCl<sub>3</sub> (0.9 mL, 10.0 mM). The solution was stirred at 0 °C for 1 h and at room temperature for another 1 h. Absolute ethanol (20 mL) solution containing 2,5-dimethoxy-N,N-diethylamino (2.4 g, 10.0 mM) was added dropwise into the mixture and refluxed at 70 °C for 12 h, then cooled to 5 °C. A solution of 20 g of sodium acetate in 200 mL of cold water was added slowly with stirring. The reaction mixture was then stirred for an additional hour and the resulting solution was extracted with diethyl ether. The combined extract was washed with saturated anhydrous NaHCO<sub>3</sub> and then washed with water. The organic layer was dried over anhydrous magnesium sulfate and the solvent was removed under reduced pressure. The residue was purified by column chromatography (hexane : ethyl acetate = 5:2) on silica gel. 1.08 g of colorless microcrystal was obtained. Yield: 51.7%.

**2-methoxy-3-diethylamino-5-methylbenzaldehyde.** 2-methoxy-3-diethylamino (0.35 g, 20 mmol), a small quantity of KI and CH<sub>3</sub>I (1.0 mL) were placed into a 20 mL. The mixture was stirred for 5 h at 60 °C, filtered and the crude product. Absolute ethanol (20 mL) solution containing crude product and treated dropwise with POCl<sub>3</sub> (0.9 mL, 10.0 mM). was added dropwise into the mixture and refluxed at 80 °C for 8 h and treated dropwise with POCl<sub>3</sub> (0.9 mL, 10.0 mM), then cooled to 5 °C, give a 2-methoxy-3-diethylamino-5-methylbenzaldehyde as powder. Yield: 51.8%.

**2-methoxy-3-diethylamino-5-nitrylbenzaldehyde.** 2-methoxy-3-diethylamino (0.35 g, 20 mmol) and hydrogen nitrate were placed into 30 mL of dry DMF. The mixture was stirred at 5 h at 70 °C, filtered and the crude product. Absolute ethanol (20 mL) solution containing crude product and treated dropwise with POCl<sub>3</sub> (1.5 mL, 15.0 mM), was added dropwise into the mixture and refluxed at 80 °C for 7 h, filtered and give a 2-methoxy-3-diethylamino-5-nitrylbenzaldehyde as powder. Yield: 48.9%

**1,7-bis[(2,5-dimethoxy-3-diethylamino)phenyl]-1,6-heptadiene-3,5-dione (Dye 1).** Potassium tertbutoxide (0.10 g, 8.0 mM) was added to a solution of acetylacetone (0.3 mL, 3.5 mM) in DMF (5 mL) and the resultant mixture was stirred at room temperature for 1 h under nitrogen atmosphere. 2,5-dimethoxy-3-(diethylamino)benzaldehyde (1.74 g, 7.0 mM) was added and the reaction mixture was stirred at 40 °C for 15 h. The reaction mixture was poured over saturated aqueous ammonium chloride and then extracted with ethyl acetate. The organic layer was washed with water and anhydrous MgSO<sub>4</sub>, respectively. The solvent was removed under reduced pressure, and the residue was purified by column chromatography (hexane : ethyl acetate = 4:3) to give Dye 1 (1.83 g) as pale yellow microcrystal. Yield: 53.8%. m.p. 152-154 °C. <sup>1</sup>H NMR (400 MHz, DMSO-d<sub>6</sub>) δ: 7.85 (d, J = 15.0 Hz, 2H), 7.46 (d, J = 12.8 Hz, 2H), 6.86-6.65 (m, 4H), 5.77 (s, 2H), 3.68-3.45 (m, 12H), 3.20-3.15 (m, 8H), 2.90 (s, 12H); <sup>13</sup>C NMR (75 MHz, DMSO-d<sub>6</sub>) δ: 190.2, 154.4, 150.2, 145.1, 132.0, 131.7, 131.4, 128.2, 125.5, 122.7, 115.9, 115.3, 88.7, 44.4, 41.7, 24.5, 21.3; MS (ESI) m/z: 539.65 ([M + H]<sup>+</sup>, 100); Anal. calcd for C<sub>31</sub>H<sub>42</sub>N<sub>2</sub>O<sub>6</sub>: C 69.12, H 7.86, N 5.20; found: C 68.89, H 7.63, N 5.06.

**1,7-bis[(2-methoxy-3-diethylamino-5-methyl)phenyl]-1,6-heptadiene-3,5-dione**

**(Dye 2).** The synthesis method of Dye 2 is similar to that of Dye 1. The compound was obtained starting from 2-methoxy-3-diethylamino-5-methylbenzaldehyde. The crude product was purified by column chromatography (ethyl acetate : petroleum ether mixture = 9:5) to get pale yellow microcrystal. Yield: 51.6%. m.p. 145-147 °C. <sup>1</sup>H NMR (400 MHz, DMSO-d<sub>6</sub>) δ: 7.78 (d, J = 15.0 Hz, 2H), 7.42 (d, J = 12.8 Hz, 2H), 6.82-6.64 (m, 4H), 5.68 (s, 2H), 3.63-3.42 (m, 12H), 3.18-3.13 (m, 8H), 2.88 (s, 12H); <sup>13</sup>C NMR (75 MHz, DMSO-d<sub>6</sub>) δ: 190.0, 154.3, 150.1, 144.9, 131.7, 131.4, 131.1, 127.9, 125.2, 122.3, 115.5, 115.0, 88.4, 44.2, 41.5, 24.1, 21.1; MS (ESI) m/z: 507.63 ([M + H]<sup>+</sup>, 100); Anal. calcd for C<sub>31</sub>H<sub>42</sub>N<sub>2</sub>O<sub>4</sub>: C 73.48, H 8.36, N 5.53; found: C 73.26, H 8.21, N 5.34.

**1,7-bis[(2-methoxy-3-diethylamino-5-nitryl)phenyl]-1,6-heptadiene--3,5-dione**

**(Dye 3).** The synthesis method of Dye 3 is similar to that of Dye 1. The compound was obtained starting from 2-methoxy-3-diethylamino-5-nitrylbenzaldehyde. The crude product was purified by column chromatography (ethyl acetate : petroleum ether mixture = 7:6) to get pale yellow microcrystal. Yield: 43.7%. m.p. 125-127 °C. <sup>1</sup>H NMR (400 MHz, DMSO-d<sub>6</sub>) δ: 7.90 (d, J = 15.0 Hz, 2H), 7.51 (d, J = 12.8 Hz, 2H), 6.92-6.71 (m, 4H), 5.83 (s, 2H), 3.71-3.50 (m, 6H), 3.23-3.15 (m, 8H), 2.94 (s, 12H); <sup>13</sup>C NMR (75 MHz, DMSO-d<sub>6</sub>) δ: 190.5, 154.7, 150.5, 145.4, 132.3, 131.9, 131.7, 128.5, 125.8, 122.9, 116.1, 115.6, 88.9, 44.7, 41.9, 24.8, 21.5; MS (ESI) m/z: 569.60 ([M + H]<sup>+</sup>, 100); Anal. calcd for C<sub>29</sub>H<sub>36</sub>N<sub>4</sub>O<sub>8</sub>: C 61.25, H 6.38, N 9.86; found: C 60.98, H 6.22, N 9.64. .

### 3. Results and discussion

#### 3.1. Preparation and characterization of Dyes 1-3

Synthetic route of as-prepared Dyes 1-3 and their intermediates are shown in Scheme 1. The high reactivity of acetyl acetone in alkaline condensation reactions with aldehyde is well-known. In the light of the mechanism from the literature [30], Dyes 1-3 were prepared by the condensation reaction between acetyl acetone and 2,5-dimethoxy-3-(diethylamino)benzaldehyde, and 2-methoxy-3-diethylamino-5-methylbenzaldehyde, and 2-methoxy-3-diethylamino-5-nitrylbenzaldehyde,

respectively. The structures of Dyes 1-3 were characterized by NMR, MS spectroscopic methods and elementary analyses, and the satisfactory analysis data were obtained (Supporting Information).

### 3.2. The photophysical properties of Dyes 1-3

The photophysical data of Dyes 1-3 are showed in Table 1. Fig. 1a displays the linear absorption spectra of Dyes 1-3 in DMF with a solution concentration of  $1.0 \times 10^{-5}$  mol/L. From Fig. 1a, one can see that the absorption behaviors of the three compounds are almost the same because of their similar structure. The three curves show that absorption maximum at 328 nm for Dye 1, 331 nm for Dye 2, and 330 nm for Dye 3, corresponding to the n- $\pi^*$  transition of the compound [31].

As expected, with introduction of terminal electron-rich donor or electron-deficient acceptor groups, these compounds exhibited a large Stokes shift (more than 130 nm) with their emission maximum (shown in Table 1), which fell in the range for NIR probes. Particularly, the compound Dye 2 displayed a largest Stokes shift ( $\lambda_{\max}(\text{ex}) = 499$  nm,  $\lambda_{\max}(\text{em}) = 635$  nm). Furthermore, by comparing the fluorescence intensity, the quantum yield of Dye 2 was significantly higher than that of curcumin and other Dyes, which may be explained by better coplanarity and the stronger electron-donating ability (methyl) of the Dye 2 molecule.

**Table 1** The optical properties of the compounds upon binding with and without A $\beta$  plaques

Compd	$\lambda$ <sup>a</sup> <sub>abs</sub> (nm)	$\epsilon^b \times$ $10^4$ (M <sup>-1</sup> c m <sup>-1</sup> )	Unbound <sup>c</sup> (free)			Bound <sup>g</sup>			Fold ( $\Phi_2/\Phi_1$ )
			$\lambda^d$ <sub>ex</sub> (nm)	$\lambda^e$ <sub>em</sub> (nm)	$\Phi_1^f$	$\lambda_{ex}$ (nm)	$\lambda_{em}$ (nm)	$\Phi_2$	
Dye 1	328	3.24	479	609	0.018	479	609	0.32	17.8
Dye 2	331	3.86	499	635	0.019	499	635	0.37	19.5
Dye 3	330	3.18	497	633	0.016	497	633	0.29	18.1
Cur	315	2.87	421	522	0.014	423	521	0.22	15.7

<sup>a</sup> absorption spectra of the compounds determined in DMF. <sup>b</sup> Molar extinction coefficient determined in DMF. <sup>c</sup> Fluorescence properties of the compounds measured in PBS in absence of A $\beta$  plaques. <sup>d</sup> Maximum excitation wavelength of the compound measured in DMF. <sup>e</sup> Maximum emission wavelength of the compound. <sup>f</sup> Quantum yield of the compound were measured in DMF. <sup>g</sup> Fluorescence property of the compound measured in PBS in presence of A $\beta$  plaques.

### 3.3. Fluorescence response of NIR probe toward A $\beta$ plaques

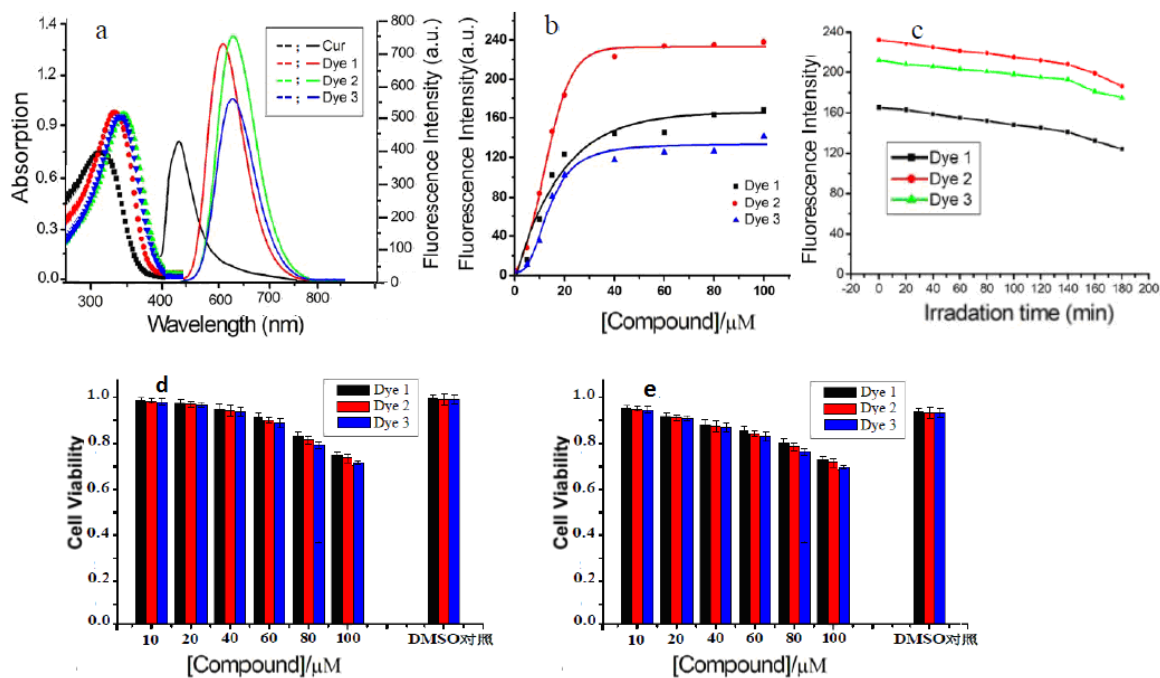
Scanning electron microscopy (SEM) had been used here to analyze the morphology of dyes (dye 1, dye 2 and dye 3). The SEM images of dyes were given in Fig.S6. The shape of the particles is regular and the particles are of variable diameter ranging from 25 to 37 nm. In phosphate buffered saline (PBS, PH = 7.2) at 37 °C, dye(dye 1, dye 2 and dye 3) remained and maintained its original compound size for up to 12 days, indicating the excellent stability of dyes probe in aqueous conditions.

Table 1 exhibited that curcumin and the Dyes 1-3 possessed significant increases of quantum yield after mixing with the A $\beta$  plaques. Curcumin showed a 15.7-fold increase in quantum yield and a Stokes shift (98 nm) in fluorescence upon binding to

A $\beta$  plaques, but the maximum emission wavelength was observed only at 521 nm. Among the compounds, Dye 2 with methoxy and methyl substituents showed the most notable fluorescence properties ( $\lambda_{em}$ , 635 nm, 136 nm of Stokes shift and 19.5-fold quantum yield increase), which indicated that it had the desired optical properties of a useful fluorescence probe for A $\beta$  plaques. However, Dyes 1 and 3 displayed relatively small increase in fluorescence intensities and quantum yields upon mixing with A $\beta$  plaques. Compared with the low fluorescence quantum yield (< 0.2%) of the free compound in DMF, the curcumin-based NIR probes exhibited significant fluorescence increase upon binding to A $\beta_{1-40}$  plaques (Supporting Information). The fluorescence enhancement might be attributed to the restricted rotation of the photo-excited dyes upon binding to A $\beta$  plaques, resulting in a large reduction in the fluorescence decay [32]. The results suggested that these dyes would be “turned on” upon interacting with a host.

On the other hand, comparison of the fluorescence spectra of NIR probes upon binding to A $\beta$  plaques provided a clue for understanding this interesting structure–property relationship. The compound with small fluorescence increases (Dye 1 and 3) shared a common feature: there is electron-withdrawing groups in the molecular structure. In particular, electron withdrawing ability of the nitril group in Dye 3 was stronger than that of methoxy group in Dye 1.

In order to quantitatively evaluate the binding affinity of Dyes 1-3 with A $\beta$  plaques, an in vitro saturation-binding assay was conducted by the fluorescence titrations and the  $K_d$  constants were measured by using saturation assays as reported previously [33]. As shown in Fig. 1b, the nonlinear curve fitting indicated that these Dyes possessed stronger binding affinities toward the A $\beta$  plaques, and the fluorescence enhancement upon binding to A $\beta$  plaques is in the order of  $F_{Dye\ 2} (K_d, 1.36\ \mu M) > F_{Dye\ 1} (K_d, 2.68\ \mu M) > F_{Dye\ 3} (K_d, 3.43\ \mu M)$ . Interestingly, Dyes 2 bound to A $\beta$  plaques more favorably than Thioflavin-S, a widely used agent for detecting protein and A $\beta$  aggregation ( $K_d$ , 1.90  $\mu M$ ) [34].



**Fig. 1.** (a) Absorption and fluorescence emission spectra of Dyes 1-3 ( $1.0 \times 10^{-5}$  mol/L). (b) Saturation binding curves of A $\beta_{1-40}$  plaques (50  $\mu\text{M}$ ) to the concentration of each dye (0-100  $\mu\text{M}$ ) (c) Fluorescence intensity changes of Dyes 1-3 during irradiation time. (d) Cytotoxicity of obtained compounds against MCF-7 cell line (24 h). (e) Cytotoxicity of obtained compounds against MCF-7 cell line (48 h) at different concentrations from the MTT assay.

### 3.5. Cytotoxicity and stability studies

In order to evaluate the potential application of Dyes 1-3, the cytotoxicity of these dyes towards human breast cancer (MCF-7) cells was evaluated using the MTT assay. Different concentrations in the range of 0-100  $\mu\text{M}$  of Dyes 1-3 were given to cells upon exposure for 24 h and for 48 h. The results were shown in Fig. 1c. No obvious cell viability decrease was observed and the cell viability ( $\leq 40$   $\mu\text{M}$ ) was still greater than 85% when the concentration of the compound reached up to 80  $\mu\text{M}$ , which is 4 times of the concentration used for cell imaging in our living cell imaging. The low cytotoxicity of the obtained target compound indicates its suitability for biological imaging applications.

We investigated too the *in vitro* stability of Dyes 1-3 in mouse plasma by

monitoring their fluorescence intensity for 3 h (Fig. 1d). Dyes 1-3 existed as a hardly degradation form, suggesting these compounds were relatively stable in mouse plasma. On the whole, Dyes 2 showed promising potential application for the imaging of A $\beta$  plaques.

### 3.6. Fluorescent staining of AD brain tissue sections

In order to assess bioimaging, Dye 2 was selected to monitor intracellular A $\beta$  plaques. Post-mortem human frontal cortex tissue from a subject diagnosed with clinical Alzheimer's disease were sliced into 5  $\mu$ m by a microtome and, and then stained with Dye 2 (20  $\mu$ M). With confocal microscopy observation, the intracellular expression of A $\beta$  plaques was confirmed by yellow green fluorescence stained with Dye 2 (Fig. 2b). It is spacing needed that the same circular vacuole-like subcellular structures were also observed when stained with the silver reagent (white arrows in Fig. 2a). In contrast, the adjacent section was uniformly stained in the negative control (normal group) (Fig. 2c). The results of the colocalization in the *in vitro* fluorescence images suggested that Dye 2 specifically detected A $\beta$  plaques in live cells.■

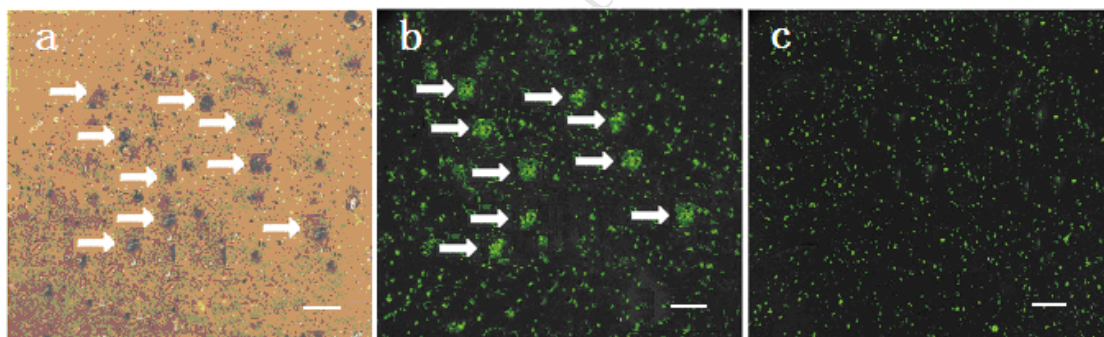


**Fig. 2.** Fluorescent staining of adjacent brain tissue sections of AD patients. a) silver staining, b) Dye 2 staining, c) the negative control. The white arrows indicate A $\beta$  plaques. The scale bars are 50  $\mu$ m.

### 3.7. Curcumin binding in control and AD brain tissue

It was observed that curcumin binding on human brain tissue presented no background staining and auto-fluorescent signals in neurons. In brain tissue of EOAD, LOAD and AD cases with CAA (CAA type 1), the compounds strongly bound to amyloid plaques and CAA (Fig. 1). Curcumin staining revealed different types of

plaques. We observed intense staining of primitive/compact plaques and moderate staining of the cores in cored plaques. In AD cases, neurofibrillary tangles (NFTs) showed a weak detection by the Dyes. Adjacent sections were assessed by immunohistochemistry for the presence of A $\beta$  and pTau in a corresponding area, which confirmed the presence of these pathological structures. The binding of the dyes to these pathological structures were investigated by co-stainings for dyes and A $\beta$  (IC-16) or pTau (AT8). Primitive/compact plaques showed almost a complete overlap of dyes signal and immunodetection by A $\beta$  (Fig. 2). Classic cored plaques presented co-labeling of the core, while the corona of these plaques were immuno-labelled by anti-A $\beta$  and not by dyes. No binding of the dyes were observed in diffuse A $\beta$  deposits. CAA affected blood vessels were stained most intensively by dyes and showed a complete overlap with the detection of CAA by A $\beta$ . While compact plaques showed moderate neuritic changes, as presented by anti-pTau immuno-labeling, no co-labelling of anti-pTau and dyes were present in these plaques (Fig. 3). Neuritic cored plaques showed a strong immunodetection of pTau around the core. The core of neuritic plaques showed a strong binding of the dyes while co-labelling with anti-pTau were absent. A strong binding of dyes were observed in CAA, however, no co-labelling with anti-pTau, observed around CAA affected capillaries, was detected. Co-labeling with anti-pTau confirmed that curcumin weakly detects NFTs, they showed slightly less apparent staining of fibrillar, primitive/compact plaques and NFTs compared to Thioflavin-S (Fig. 2).

### 3.8. In vivo imaging

To investigate whether Dye 2 had the capacity to detect A $\beta$  plaques in the mouse brain, APP/PSI mice, which most studied transgenic AD mouse model [35,36], were used as a NIR imaging of Dye 2. Previous reports shown that the APP/PSI mouse carried double humanized APP/PSI genes and develops significant amyloid plaques and displays memory deficits around 10 - 12 months of age [24,37]. In this studied, we use 17- month of age mouse model for *in vivo* NIR imaging. As shown in Fig. 3, one can be seen that the A $\beta$  plaques site was recognizable within 1 h after injection of the compound Dye 2. Interestingly, as time progresses, the probe increasingly accumulated in the A $\beta$  plaques and the fluorescence reached the highest intensity at

about 2 h after injection. However, the fluorescence in the A $\beta$  plaques position began to wear off, and then the fluorescence almost completely disappeared from the A $\beta$  plaques at about 4 h after injection. The results suggest that the compound is able to detect the A $\beta$  plaques in AD.

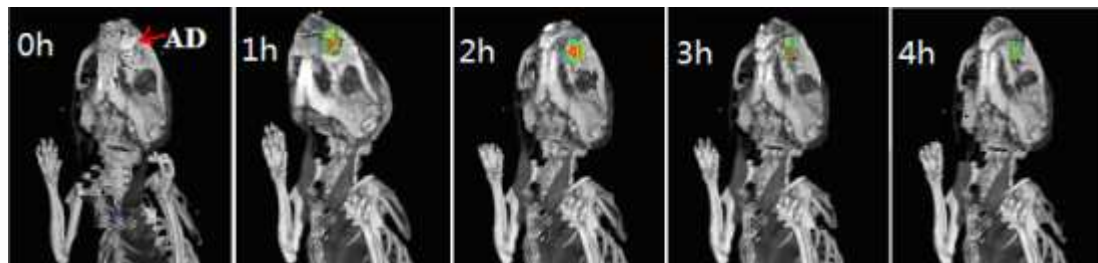


**Fig. 3.** Representative images of APP/PSI mice and control littermates at different time points before and after intravenously injection with Dye 2

#### 4. Conclusions

In summary, three curcumin-based NIR dyes 1-3 for A $\beta$  plaques were synthesized which exhibited obvious fluorescence enhancement after binding to A $\beta$  plaques. Interestingly, Dye 2 with methoxy and methyl substituents shows the intense fluorescence, low cytotoxicity and high quantum yield, good stability in mouse serum, as well as fluorescent imaging of A $\beta$  plaques reveal its potentially suitable for use in the early diagnoses of A $\beta$  plaques.

#### Acknowledgements

This research was financially supported by the National Natural Science Foundation of China (No. 21071001), The Natural Science Foundation of Anhui Province (No. 1808085MB47), Department of Education Committee of Anhui Province and the Center for Anhui Province Engineering of Modern Chinese traditional medicine (No. KJ2017A291), and the Opening Foundation of Anhui Province Key Laboratory of Environment-friendly Polymer Materials (No. 2018001)..

#### References

- [1] J. Hardy, D.J. Selkoe, The amyloid hypothesis of Alzheimer's disease: progress and problems on the road to therapeutics. *Science* 2002, 297: 353–356.

- [2] J. Praet, C. Bigot, J. Orije, M. Naeyaert, D. Shah, Magnetization transfer contrast imaging detects early white matter changes in the APP/PS1 amyloidosis mouse model. *NeuroImage: Clinical* 2016, 12: 85–92.
- [3] L. Zhu, K. Ploessl, H.F. Kung, PET/SPECT imaging agents for neurodegenerative diseases. *Chem. Soc. Rev.* 2014, 43: 6683-6691.
- [4] Y. Cheng, M. Ono, H. Kimura, M. Ueda, H. Saji, Technetium-99m labeled pyridyl benzofuran derivatives as single photon emission computed tomography imaging probes for beta-amyloid plaques in Alzheimer's brains. *J. Med. Chem.* 2012, 55: 2279-2286.
- [5] S. Li, H. He, W. Cui, B. Gu, J. Li, Z. Qi., Detection of A $\beta$  plaques by a novel specific MRI probe precursor CR-BSA-(Gd-DTPA)<sub>n</sub> in APP/PS1 transgenic mice. *Adv. Integr. Anat. Evol. Biol.* 2010, 293: 2136-2143.
- [6] Di Wu, Yuanzhi Shen, Jianhua Chen, Guotao Liu, Haiyan Chen, Jun Yin, Naphth-alimide-modified near-infrared cyanine dye with a large stokes shift and its application in bioimaging, *Chin. Chem. Lett.* 2017, 28, 1935-1942.
- [7] Zhiqiang Xu, Jianhua Chen, Liu-Li Hu, Ying Tan, Sheng-Hua Liu, Jun Yin, Recent advances in formaldehyde-responsive fluorescent probes, *Chin. Chem. Lett.* 2017, 28, 1935-1942.
- [8] Yanzhu Liu, Liucheng Mao, Saijiao Yang, Meiyong Liu, Hongye Huang, Yuanqing Wen, Fengjie Deng, Yongxiu Li, Xiaoyong Zhang, Yen Wei, Synthesis and biological imaging of fluorescent polymeric nanoparticles with AIE feature via the combination of RAFT polymeric nanoparticles polymerization modification, *Dyes and Pigments*, 2018, 158, 79-87.
- [9] Ruming Jiang, Meiyong Liu, Hongye Huang, Long Huang, Qiang Huang, Yuanqing Wen, Qianyong Cao, Jianwen Tian, Xiaoyong Zhang, Yen Wei, Microwave-assisted multicomponent tandem polymerization for rapid preparation of biodegradable fluorescent organic nanoparticles with aggregation-induced emission feature and their biological imaging applications *Dyes and Pigments*, 2018, 149, 581-587,
- [10] Hongye Huang, Meiyong Liu, Qing Wan, Ruming Jiang, Dazhuang Xu, Qiang

Huang, Yuanqing Wen, Fengjie Deng, Xiaoyong Zhang, Yen Wei, Facile fabrication of luminescent hyaluronic acid with aggregation-induced emission through formation of dynamic bonds and their theranostic applications, *Materials Science and Engineering: C*, 2018, 91, 201-207

[11] Ruming Jiang, Han Liu, Meiyong Liu, Jianwen Tian, Qiang Huang, Hongye Huang, Yuanqing Wen, Qianyong Gao, Xiaoyong Zhang, Yen Wei, A facile one-pot Mannich reaction for the construction of fluorescent polymeric nanoparticles with aggregation-induced emission feature and their biological imaging, *Materials Science and Engineering: C*, 2017, 81, 416-421.

[12] Xiaoyong Zhang, Shiqi Wang, Liangxin Xu, Lin Feng, Yan Ji, Lei Tao, Shuxi Li and Yen Wei, Biocompatible polydopamine fluorescent organic nanoparticles: facile preparation and cell imaging, *Nanoscale*, 2012, 4 (18), 5581-5584.

[13] G.Y. Xu, D. Wei, J.F. Wang, B. Jiang, M.H. Wang, X. Xue, S.S. Zhou, B.X. Wu, M.H. Jiang, Crystal structure, optical properties and biological imaging of two curcumin derivatives. *Dyes Pigments*, 2014, 101: 312–317.

[14] U. Subudhi, K. Das, B. Paital, S. Bhanja, G.B.N. Chainy, Supplementation of curcumin and vitamin E enhances oxidative stress, but restores hepatic histoarchitecture in hypothyroid rats. *Life Sciences* 2009, 84: 372-379.

[15] Zhiqiang Xu, Xiaoting Huang, Xie Han, Di Wu, Bibo Zhang, Ying Tan, Meijiao Gao, Shenghua Liu, Jun Yin, Juyoung Yoon, A visible and Near-infrared, Dual-Channel Fluorescence on probe for Selectively Tracking Mitochondrial GI Utathione, *Chem* 2018, 7, 1609-1628

[16] S.S. Zhou, X. Xue, J.F. Wang, B. Jiang, D. Wei, Y. Jia, Synthesis, optical properties and biological imaging of the rare earth complexes with curcumin and pyridine. *J. Mater. Chem.* 2012, 22: 22774–22780.

[17] M. Garcia-Alloza, L.A. Borrelli, A. Rozkalne, B.T. Hyman and B.J. Bacskai, Curcumin labels amyloid pathology in vivo, disrupts existing plaques, and partially restores distorted neuritis in an Alzheimer mouse model. *J. Neurochem.* 2007, 102: 1095-1101.

[18] F. Yang, G.P. Lim, A.N. Begum, O.J. Ubeda, M.R. Simmons, S.S. Ambegaokar,

- P.P. Chen, R. Kaye, C.G. Glabe, S.A. Frautschy and G.M. Cole, Curcumin inhibits formation of amyloid beta oligomers and fibrils, binds plaque, and reduces amyloid in vivo. *J. Biol. Chem.* 2005, 280: 5892-5898.
- [19] K.S. Park, Y. Seo, M.K. Kim, K. Kim, Y.K. Kim, H. Choob and Y. Chong, A curcumin-based molecular probe for near-infrared fluorescence imaging of tau fibrils in Alzheimer's disease. *Org. Biomol. Chem.* 2015, 13: 11194–11199.
- [20] M. Albota, D. Beljonne, L. Brédas, J.E.J. Ehrlich, J.Y. Fu, A.A. Heikal, S.E. Hess, T. Kogej, M.D. Levin, S.R. Marder, D. McCord-Maughon, J.W. Perry, H. Rckel, M. Rumi, C. Subramaniam, W.W. Webb, X.L. Wu and C. Xu, *Science* 1998, 281: 1653–1655.
- [21] M. Rumi, J.E. Ehrlich, A.A. Heikal, J.W. Perry, S. Barlow, Z. Hu, D. McCord-Maughon, T.C. Parker, H. Rckel, S. Thayumanavan, S.R. Marder, D. Beljonne and J.L. Breddas, Structure–Property Relationships for Two-Photon Absorbing Chromophores: Bis-Donor Diphenylpolyene and Bis(styryl)benzene Derivatives *J. Am. Chem. Soc.* 2000, 122: 9500–9510.
- [22] C. Ran, X. Xu, S.B. Raymond, B.J. Ferrara, K. Neal, B.J. Bacskai, Z. Medarova and A. Moore, Design, synthesis, and testing of difluoroboron-derivatized curcumins as near-infrared probes for in vivo detection of amyloid- $\beta$  deposits. *J. Am. Chem. Soc.* 2009, 131: 15257-1562.
- [23] X. Zhang, Y. Tian, Z. Li, X. Tian, H. Sun, H. Liu, A. Moore and C. Ran, Design and synthesis of curcumin analogues for in vivo fluorescence imaging and inhibiting copperinduced cross-linking of amyloid beta species in Alzheimer's disease. *J. Am. Chem. Soc.* 2013, 135: 16397-16401.
- [24] W.E. Klunk, Y.M. Wang, G.F. Huang, M.L. Debnath, D.P. Holt, C.A. Mathis, Uncharged thioflavin-T derivatives bind to amyloid-beta protein with high affinity and readily enter the brain. *Life science* 2001, 68: 1471-1484.
- [25] D.D. Nan, C.S. Gan, C.W. Wang, J.P. Qiao, X.M. Wang, J.N. Zhou, 6-Methoxy-indanone derivatives as potential probes for  $\beta$ -amyloid plaques in Alzheimer's disease. *European Journal of Medicinal Chemistry* 2016, 124: 117-128.
- [26] C.Z. Ran, X.Y. Xu, S.B. Raymond, B. J. Ferrara, K. Neal, B. J. Bacskai, Z.

- Medarova, A. Moore, Design, synthesis, and testing of difluoroboron derivatized curcumins as near infrared probes for in vivo detection of amyloid- $\beta$  deposits, *J. Am. Chem. Soc.* 2009, 131(42): 15257–15261.
- [27] Xiaoyong Zhang, Ke Wang, Meiyong Liu, Xiqi Zhang, Lei Tao, Yiwang Chen and Yen Wei, Polymeric AIE-based nanoprobe for biomedical applications: recent advances and perspectives, *Nanoscale*, 2015, 7 (27), 11486-11508.
- [28] G.Y. Xu, J.F. Wang, T. Liu, M.H. Wang, S.S. Zhou, M.H. Jiang, Synthesis and crystal structure of a novel copper(II) complex of curcumin-type and its application in in vitro and in vivo imaging, *J. Mater. Chem. B*, 2014, 2, 3659 - 3666.
- [29] C.Z. Ran, X.Y. Xu, S.B. Raymond, B. J. Ferrara, K. Neal, B. J. Bacsikai, Z. Medarova, A. Moore, Design, synthesis, and testing of difluoroboron derivatized curcumins as near infrared probes for in vivo detection of amyloid- $\beta$  deposits, *J. Am. Chem. Soc.* 2009, 131(42): 15257–15261.
- [30] H. Chao, R.H. Li, C.W. Jiang, H. Li, L.N. Ji and X.Y. Li, Mono-, di- and tetra-nuclear ruthenium(II) complexes containing 2,2'-*p*-phenylenebis(imidazo[4,5-*f*]phenanthroline): synthesis, characterization and third-order non-linear optical properties. *J. Chem. Soc., Dalton Trans.*, 2001, 1920-1926.
- [31] C.Z. Ran, X.Y. Xu, S.B. Raymond, B.J. Ferrara, K.N. Brian, Z. Medarova, and A. Moore, Design, synthesis, and testing of difluoroboron derivatized curcumins as near infrared probes for in vivo detection of amyloid- $\beta$  deposits. *J. Am. Chem. Soc.* 2009, 131(42): 15257–15261.
- [32] H.P. Zhou, D.M. Li, J.Z. Zhang, Y.M. Zhu, J.Y. Wu, Z.J. Hu, Crystal structures, optical properties and theoretical calculation of novel two-photon polymerization initiators. *Chem. Phys.* 2006; 322: 459-470.
- [33] H.J. Tong, K. Loua, W. Wang, Near-infrared fluorescent probes for imaging of amyloid plaques in Alzheimer's disease. *Acta Pharmaceutica Sinica B* 2015, 5(1): 25–33.
- [34] Y.H. Li, D. Xu, S.L. Ho, H.W. Li, R.H. Yang, A theranostic agent for in vivo near-infrared imaging of  $\beta$ -amyloid species and inhibition of  $\beta$ -amyloid aggregation.

Biomaterials 2016, 94: 84-92.

[35] B. Delalour, M. Guegan, A.Volk, M. Dhenain, Neurobiology of aging, 2006, 27: 835-839.

[36] X.L. Zhang, Y.L. Tian, Z. Li, X.Y. Tian, A. Moore, C.Z. Ran, Design and synthesis of curcumin analogues for in vivo fluorescence imaging and inhibiting copper-induced cross linking amyloid beta species in Alzheimer's disease. J. Am. Chem. Soc. 2013, 135 (44): 16397 – 16409.

[37] Hsiao K, Chapman P, Nilsen S, Eckman C, Harigaya Y, Younkin S, Yang F, Cole G. Correlative memory deficits, A beta elevation, and amyloid plaques in transgenic mice. Science 1996, 274: 99–102.

**Research highlights**

- \* Three novel compounds curcumin-based was synthesized
- \* These compounds shown obvious fluorescence change after binding to A $\beta$  plaques.
- \* These compounds have Cytotoxicity..
- \* Imaging strained with Dye 2 confirmed that it could be to detect A $\beta$  plaques in AD.